Available online at www.sciencedirect.com
ScienceDirect
Scripta Materialia 59 (2008) 1167–1170
Scripta MATERIALIA
www.elsevier.com/locate/scriptamat

In situ SANS investigation of the kinetics of rafting of γ′ precipitates in a fourth-generation single-crystal nickel-based superalloy

N. Ratel,[a,b,*] B. Demé,[a] P. Bastie[a,b] and P. Caron[c]

[a] *Institut Laue Langevin, 6 rue Jules Horowitz, BP 156, 38042 Grenoble Cedex, France*
[b] *Laboratoire de Spectrométrie Physique, UMR CNRS No. 5588, BP 87, 38402 Saint Martin d'Hères Cedex, France*
[c] *ONERA, BP 72, 29, Avenue de la Division Leclerc, 92322 Châtillon Cedex, France*

Received 13 May 2008; revised 17 July 2008; accepted 18 July 2008
Available online 3 August 2008

Rafting of the γ′ particles in the fourth-generation single-crystal nickel-based superalloy MC-NG was investigated in situ using small-angle neutron scattering. Rafting was induced by high-temperature annealing of a predeformed sample in the absence of applied stress. The use of extended Porod's approximation allowed the investigation of the specific area evolution during the microstructure change. By comparison with a first-generation alloy, it is found that the alloy composition does not seem to influence the kinetics of rafting.

Keywords: Nickel alloys; Small-angle neutron scattering; Strain-induced rafting

Single-crystal nickel-based superalloys are widely used in aircraft engines since they show good mechanical properties at high temperatures. These particularities arise from the presence of two phases: a disordered face-centred cubic γ matrix in which is embedded a high volume fraction (around 70%) of ordered $L1_2$ γ′-Ni_3Al-based precipitates. After the so-called standard heat treatment [1], the γ′ particles adopt a cuboidal shape with {100} faces and are almost periodically arranged along the ⟨100⟩ crystallographic directions. However, experimental observations have shown that the particles' morphology changes from cuboid to platelet (or raft) if a deformed material is annealed at high temperature [2]. This morphology change, also called rafting, was shown to be discriminated by plastic deformation and by the sign of the lattice parameter mismatch between γ and γ′ phases [3,4]. This microstructure evolution was first observed in samples that were deformed during a creep test at very high temperature (typically 1050 °C and 100 MPa).

Recently, the introduction of refractory elements such as rhenium (Re) and ruthenium (Ru) in new-generation nickel-based single-crystal superalloys such as MC-NG has led to improved mechanical properties in terms of creep behaviour, as compared with first-generation alloys such as AM1 [5]. The compositions of both alloys are compared in Table 1. In the MC-NG alloy, the formation of a raft microstructure appears to be retarded with respect to AM1 [1]. This delay can be attributed to the presence of an incubation period and/or the slower kinetics of rafting. In the present work, the kinetics of rafting is investigated by means of small-angle neutron scattering (SANS) in order to separate the possible influence of the refractory elements addition and of the dislocations on the microstructure evolution which occurs in the early stages of a creep test.

Two MC-NG single-crystal specimens with axes close to a ⟨001⟩ direction were provided by SNECMA and strained in tension along [001] at 850 °C with a strain rate of $1.1 \times 10^{-4}\,s^{-1}$. Their microstructure consists in a pseudo-periodical arrangement of cuboidal precipitates, as shown in Figure 1. The arrangement of the particles appears to be less organized in the MC-NG than in the AM1 alloy [5]. The plastic strains introduced in specimens 1 and 2 were 0.2% and 0.6%, respectively. The Laue X-ray diffraction technique was used to determine

* Corresponding author. Present address: Institut Laue Langevin, 28 rue Dupy du Grez, BP 156, 31300 Toulouse, France; e-mail: nicoperou@hotmail.com

1359-6462/$ - see front matter © 2008 Acta Materialia Inc. Published by Elsevier Ltd. All rights reserved.
doi:10.1016/j.scriptamat.2008.07.031

Table 1. Chemical compositions (wt.%) of the AM1 and MC-NG superalloys [5]

Alloy	Cr	Co	W	Mo	Re	Al	Ti	Ta	Hf	Others	Density (g/cm^3)
AM1	7.8	6.5	5.7	2	–	5.2	1.1	7.9	–	–	8.6
MC-NG	4	–	5	1	4	6	0.5	5	0.1	0.1 Si, 4 Ru	8.75

The Ni content balances the whole composition.

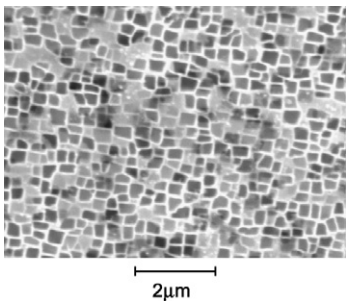

Figure 1. SEM observation of the MC-NG microstructure before annealing (white: γ; black: γ').

precisely the orientations of the $\langle 001 \rangle$ crystallographic axes for each specimen.

The change in morphology of the γ' particles which occurs during rafting has been examined in detail using the SANS technique. In situ high-temperature annealing of a deformed sample was carried out under vacuum and viewed with the V4 pinhole camera at the Hahn Meitner Institut [6]. Successive SANS spectra were acquired during the annealing. In this way, the average morphology of the γ' particles has been characterized in situ at each step of the particle morphology change. The associated kinetics was also identified.

In order to avoid multiple scattering, which may occur in thick specimens, thin slices (1.5 mm thickness) parallel to the [001] axis and normal to the [010] axis were cut from each deformed specimen by spark erosion. Each sample was then mounted in a boron nitride (neutron absorber) diaphragm (1 cm wide and 0.4 cm high) and placed in a high-temperature furnace. The [010] crystallographic direction was placed parallel to the neutron beam. During annealing, successive SANS patterns were acquired. The total in situ annealing time was around 15 h for both samples. As the [010] axis is parallel to the neutron beam, the SANS patterns contain the scattering contributions from (100) and (001) γ/γ' interfaces. The annealing temperatures were 1100 and 1050 °C for specimens 1 and 2, respectively.

In a SANS experiment, the scattering vector $\vec{q} = \vec{k_f} - \vec{k_i}$, where $\vec{k_i}$ and $\vec{k_f}$ are the incident and scattered wave vectors, respectively, has to be chosen with respect to the size of the inhomogeneities in the investigated sample. In the case of single-crystal Ni superalloys, which contain chemical inhomogeneities whose size is a few hundredths of a nanometre, the q range should be in the order of 10^{-4}–10^{-3} Å^{-1}. However, the absence of periodic arrangement of the particle observed in the MC-NG alloy leads to the absence of the correlation peak usually observed in [7]. The position of the correlation peaks provides information on the inter-particle distance, thus allowing the investigation of the microstructure evolution. The investigation of the rafting kinetics was therefore performed in a higher q range (10^{-2}–10^{-1} Å^{-1}), allowing the use of Porod's approximation [8]. In this way, the microstructure evolution that occurs during rafting was examined through the determination of the specific area of the particle/matrix interfaces.

In both specimens, the neutron wavelength was 6 Å and the sample-to-detector distance was 16 m to allow the smallest q range attainable (0.02–0.2 Å^{-1}) to be explored without too much loss of neutron flux. After annealing, SANS patterns with $\lambda = 19$ Å were recorded so as to widen the investigated q range towards lower q-values for the analysis of the final microstructure. After sufficient ageing time, γ' platelets (or rafts) are expected to form perpendicular to the [001] tensile axis. The SANS signal is therefore expected to decrease in the low q range along the [100] and/or [010] direction. The experimental data were reduced using BerSANS software [9]. The data were averaged along the [100] and [001] crystallographic directions using rectangular masks.

Figure 2 shows the rough two-dimensional SANS patterns of sample 1 acquired before and after 20 h of high-temperature annealing. Similar results were obtained in the case of sample 2 after 15 h of annealing at 1050 °C. The fourfold symmetry, with extensions along the [100] and [001] crystal directions, observed on the SANS pattern obtained at room temperature prior to annealing is representative of the cuboidal shape and of the spatial arrangement of the γ' precipitates after the standard heat treatment. The fourfold symmetry seems to become twofold after the high-temperature annealing, as shown in Figure 1b. The scattering pattern appears to be concentrated towards the low q-values, with smaller scattering branches. This phenomenon indicates that coarsening of the particles took place. On the other hand, the SANS intensity seems to decrease along the [100] direction during annealing. This result could indicate a directional γ' particle coarsening of type N, which results in a lamellar γ/γ' structure normal to the tensile axis. As the lattice parameter mismatch is negative in the investigated alloy [10] and a tensile plastic strain was introduced, the resulting microstructure corresponds to the expectations. This result is confirmed by scanning electron microscopy (SEM) observations performed after the high-temperature annealing on both specimens used in the SANS experiment, as shown in Figure 3.

Figures 4 and 5 show the scattering intensity against the scattering vector (I(q)) after data reduction and calibration obtained for specimens 1 and 2, respectively, before and after the high-temperature annealing and along the [100] and [001] directions. By comparison between the two figures, we observe that, in both specimens and before the annealing, the scattered intensities

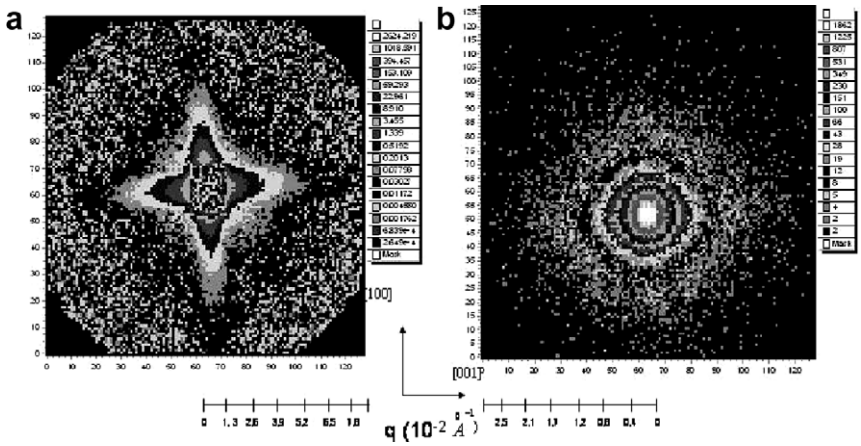

Figure 2. SANS patterns obtained in sample 1 (a) before annealing at room temperature ($\lambda = 6$ Å, $0.002 < q < 0.08$ Å^{-1}) and (b) after 20 h of annealing at 1100 °C ($\lambda = 19$ Å, $0.002 < q < 0.03$ Å^{-1}).

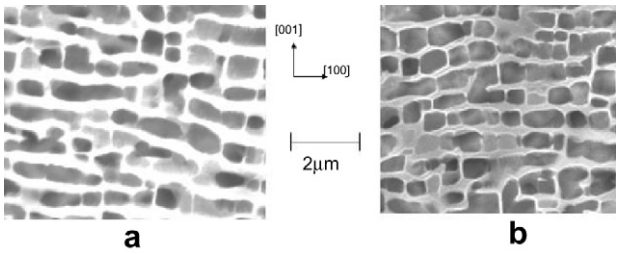

Figure 3. SEM observation of the microstructure obtained after high-temperature annealing (white: γ; black: γ′): (a) specimen 1; (b) specimen 2.

along the [1 0 0] and [0 0 1] directions show a similar q^{-4} behaviour, which is typical of a cuboidal particle shape [11]. Furthermore, the scattered intensity along [0 0 1] remains constant throughout the thermal treatment in both specimens. However, after the high-temperature annealing, the scattered intensity along the [1 0 0] direction seems to be smaller than before annealing in the low q-value range (Figures 4b and 5b). The observed asymmetric behaviour of the scattered intensity is the signature of a morphology change of the γ′ precipitates from a cuboidal shape to that of a platelet normal to the [0 0 1] crystallographic axis.

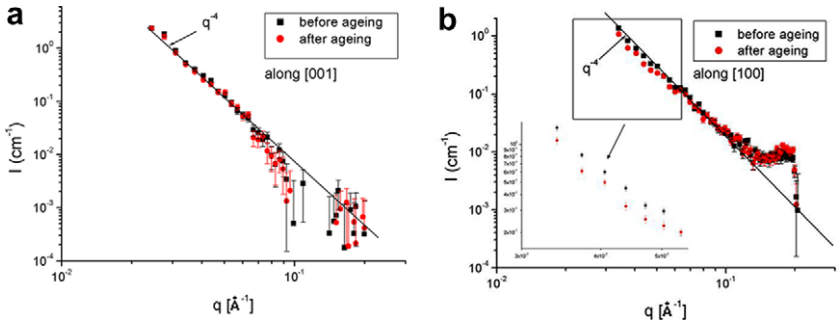

Figure 4. Normalized $I(q)$ curve for sample 1 (0.2% plastic strain, $T = 1100$ °C): (a) along [0 0 1]; (b) along [1 0 0].

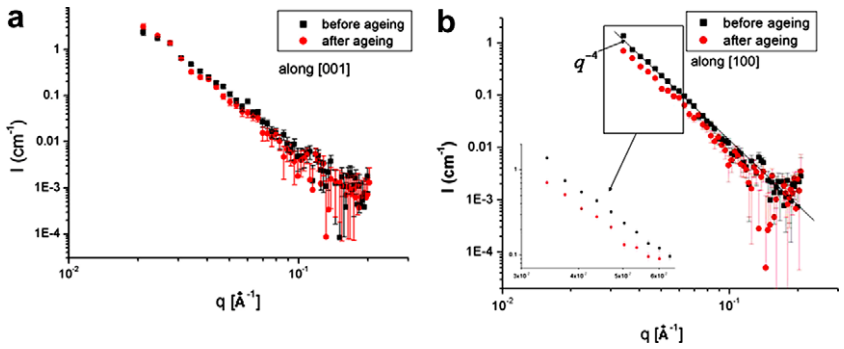

Figure 5. Normalized $I(q)$ curve for sample 2 (0.6% plastic strain, $T = 1050$ °C): (a) along [0 0 1]; (b) along [1 0 0].

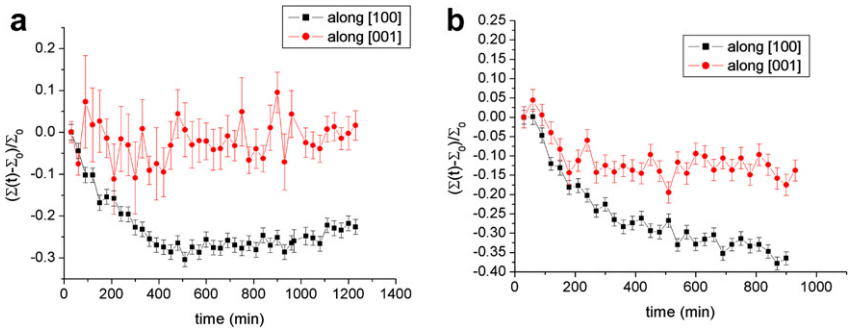

Figure 6. Evolution of the relative change in specific area with annealing time: (a) specimen 1; (b) specimen 2.

As the investigated q range corresponds to the Porod's regime, the scattered intensity, which is averaged in angular sectors where the signal is assumed to be isotropic, is related to the specific area. Figure 6 shows the evolution of the relative change in specific surface area with the annealing time for both samples and for the (100) and (001) γ/γ' interfaces. The relative change in specific area is defined as follows:

$$\frac{\Delta\Sigma(t)}{\Sigma_0} = \frac{\Sigma(t) - \Sigma_0}{\Sigma_0} \tag{1}$$

where Σ_0 is the specific area determined at the beginning of the annealing ($t = 0$), and $\Sigma(t)$ is that obtained at the time t of the high-temperature annealing.

In each sample, the specific area of the (001) interfaces remains almost constant throughout the whole annealing.

The decrease in the specific area of the (100) interfaces is clearly visible. In both specimens, this decrease can be fitted with an exponential decay with similar time constants (time constants of 274 ± 78 min and 231 ± 21 min, respectively). As temperature does not affect the diffusion processes involved in the microstructure evolution, we can consider the role of plastic strain, which is larger in specimen 2 than in specimen 1. We can reasonably speculate that the dislocations created during plastic deformation and/or vacancies provide fast diffusion paths for the atomic diffusion involved in rafting.

Moreover, if these results are compared with those from a similar experiment carried out on the AM1 alloy [12], we can see that the kinetics of rafting is comparable to that observed in MC-NG. Véron and Bastie found that the microstructure evolution was completed after around 8 h of ageing at 1100 °C in a AM1 specimen that was plastically deformed up to 0.2%. We can deduce from this remark that the diffusion processes involved in rafting do not seem to depend even on the alloy composition. This confirms the crucial role of plastic strain and associated dislocations and/or vacancies in the diffusion processes involved in strain-induced rafting.

The kinetics of γ' phase rafting was investigated in situ using small-angle neutron scattering during high-temperature annealing of deformed specimens of the MC-NG nickel-based superalloy. The use of Porod's approximation allowed us to follow the microstructure evolution through the high-temperature annealing during which rafting occurs. Comparing these results with those formerly obtained for another alloy leads to the conclusion that the addition of heavy refractory elements to an alloy does not seem to affect the kinetics of rafting. This point is explained by the role of dislocations and/or vacancies in the diffusion mechanisms involved in rafting, through the pipe diffusion process and/or the vacancy diffusion mechanism.

This research project has been supported by the European Commission under the 6th Framework Programme through the Key Action: Strengthening the European Research Area, Research Infrastructures, Contract No. RII3-CT-2003-505925 (NMI3).

[1] P. Caron, T. Khan, Mater. Sci. Eng. 61 (1983) 173.
[2] M. Véron, Y. Bréchet, F. Louchet, Acta Mater. 44 (1996) 3633.
[3] J.Y. Buffière, M. Ignat, Acta Metall. Mater. 43 (1995) 1791.
[4] N. Ratel, G. Bruno, P. Bastie, T. Mori, Acta Mater. 54 (2006) 5087.
[5] F. Diologent, Ph.D. Thesis, Université Paris XI Orsay, 2002.
[6] Available from: <http://www.hmi.de/bensc/instrumentation/instrumente/v4/v4_en.htm/>.
[7] N. Ratel, Ph.D. Thesis, Université Grenoble 1, France 76, 2007.
[8] G. Porod, Kolloid Z. 124 (1951) 83.
[9] U. Keiderling, Appl. Phys. A74 (Suppl.) (2002) S1455–S1457.
[10] F. Diologent et al., Nucl. Instrum. Meth. Phys. Res. B 200 (2003) 346–351.
[11] D. Bellet, P. Bastie, J. Lajzerowicz, J.F. Legrand, R. Bonnet, J. Phys. I 2 (1992) 205–220.
[12] M. Véron, P. Bastie, Acta Mater. 45 (8) (1997) 3277–3282.